

Laboratory Test System Design for Star Sensor Performance Evaluation

Jun Yang, Bin Liang, Tao Zhang, Jingyan Song and Liangliang Song
 Department of Automation, Tsinghua University, Beijing, China
 Email: jun-yang07@mails.tsinghua.edu.cn
 {bliang, taozhang, jysong}@mail.tsinghua.edu.cn
 Songll08@mails.tsinghua.edu.cn

Abstract—A novel laboratory test system is designed to evaluate the performance of star sensors. Two evaluation methods are presented, the star images simulation test and the zenith observation experiments method. In star image simulation, the nebula and moon lights enter into the CCD field of view (FOV) is considered. A new algorithm for fast access star catalog is also designed to enhance the speed of star image simulation. Zenith observation provides a new method to test accuracy of star sensor without telescope. The results demonstrate that the test system is effectively to evaluate the star pattern recognition rates and relatively accuracy performance of star sensors.

Index Terms—Star sensor, Star image simulation, Zenith observation, Catalog, FOV

I. INTRODUCTION

With the booming of the space exploring, accuracy attitude determination and autonomous navigation becomes the crucial requirements of the spacecrafts. Star sensors can meet both of requirements above and its accuracy is much higher than other sensors, such as sun sensor, gyroscope, magnetometer, horizon sensor and etc [1]. Star sensors have been widely used to provide high accuracy attitude for the spacecrafts missions. With the extending complication of missions, low-mass, low-cost, high-performance star sensors were developed. According to different requirements of missions, many organizations have investigated various kinds of star sensors for different applications in the last three decades. Cassini star sensor was designed for long time deep space probe by JPL [2]. The ASC star sensor was developed to deliver an accurate absolute attitude reference via a serial line to guide the telescope [3]. The StarNav star sensor was developed to validate a new ‘Lost in space algorithm’ (LISA) for determining precise spacecraft attitude without prior knowledge of position [4]. The Altair HB star sensor was developed by Surrey Satellite Technology Limited, which is a commercial star sensor employing maximum use of commercial off the shelf components [5]. All star sensors described above needed Laboratory Test systems to evaluate star sensor’s

reliability and performance after their software and hardware design completed.

The test systems can be divided into two types. One is the star image simulation test system and another is the semi-physical test system. Star image simulation test system not use the real sky picture but use the simulated star image by software. It can test the star recognition rates and stability of software in star sensor [6,7,8]. The semi-physical test system takes picture from the real sky to test the star sensor. It can test the accuracy of attitude provided by the star sensors [3,4,5]. Both of the test systems should be completed to test the star sensors.

In this paper, we design a novel laboratory test system to evaluate the performance of star sensor, including the star image simulation and semi-physical test system. In the star image simulation test system, the nebula and moon lights entering into the CCD FOV is taken into account. We also proposed a new algorithm for fast accessing the star catalog to accelerate the speed of star image simulation. In the semi-physical test system, we proposed a new zenith method to test the accuracy of the star sensor without using telescope. Experiments result show that our Laboratory test system can evaluate the star recognition rates and accuracy of star sensor effectively.

II. THE PRINCIPLE OF THE LABORATORY TEST SYSTEM

Before we design the Laboratory test system, we should know the principle of star sensor. The star sensor is composed of the optical system and the electronic processing system. The optical system is composed of the lens, the CCD (or APS) detector plane and the baffle. It takes the photos from the real sky. The electronic processing system received the digital information of the picture from the optical system, and then used the software to calculate the attitude of the spacecraft. It included the star position estimation model, the star recognition model, the attitude determination model and the tracking model. The software flow of the star sensor is shown in Figure 1.

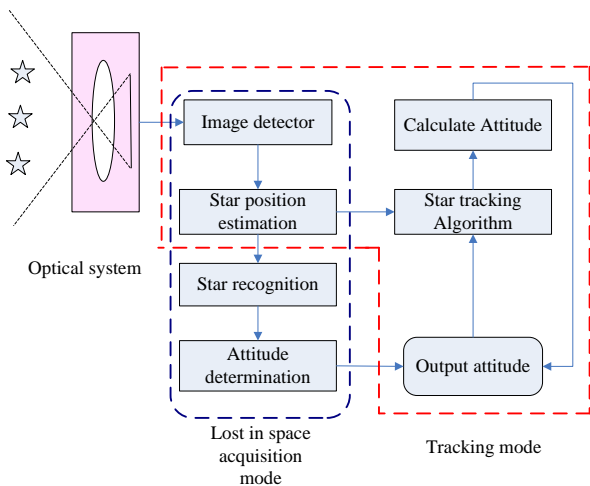


Figure 1 Software process flow of the star sensor

From the Fig. 1, the star sensor uses the optical system to capture stars from the real sky firstly. Then, it uses the star position estimation model to calculate the star positions on the CCD plane. The star recognition method is used to identify the stars from star image. It matches the pattern constructed by the stars in the real star image with a catalog of reference stars pattern stored onboard to complete the identification. Finally, the attitude determination model uses the indentified star vectors to calculate the attitude of spacecraft. A star sensor usually operates in two modes: The Lost in Space Acquisition (LISA) mode and tracking mode. The difference between these two modes is whether a prior attitude is provided. In the LISA mode, star sensor uses the star recognition algorithm to get the initial attitude. When the initial attitude is given, the star sensor enters the tracking mode.

After the star sensor software and hardware design is completed, it is necessary to establish a laboratory test system to test the performance of the star sensor. From the Fig. 1, it is seen that the input of the star sensor is the star image. So the key point of the laboratory test system is provided a star image with known attitude pointing. The principle of the laboratory test system is described in Figure 2.

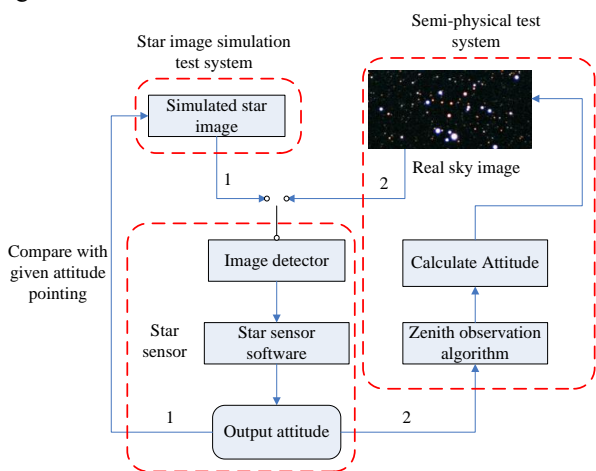


Figure 2 The frame of laboratory test system for star sensor

From the Fig. 2, we can see that the laboratory test system includes two parts, the star image simulation and

semi-physical test system. Star image simulation test system can provide simulated images in random directions with given attitude. Then the star sensor process the simulated star images and calculates the attitude of them. Compared the given attitude and the calculated attitude, we can test the star recognition rates of the star sensor. The semi-physical test system is designed for night sky experiments of the star sensor. Night sky experiments usually use the high accuracy telescope to point one direction and fixed the star sensor on it to calculate the attitude of the direction pointed by telescope. The semi-physical test system can test the accuracy of the star sensor. Under the condition of without telescope, we proposed a new zenith observation method to test the accuracy of star sensor.

III. STAR IMAGE SIMULATION TEST SYSTEM

The star image simulation test system aims to provide star images under given attitude pointing. It consists of four main parts, searching star catalog, coordinate transformation, star magnitude simulation and the noise simulation part. The frame of the star image simulation is shown in Figure. 3.

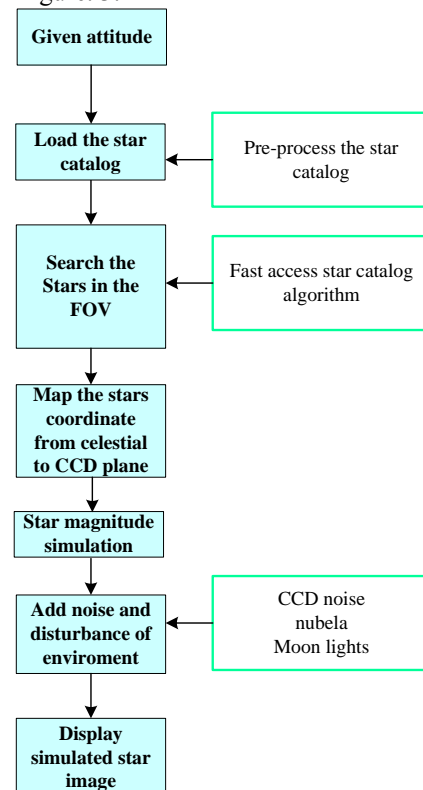


Figure 3 The frame of star image simulation

A. Star catalog accessing algorithm

When given the attitude pointing, we should find the stars in the field of view (FOV) under this pointing. We use the SKYMAP 2000 version 4 (developed by the NASA's Goddard Space Flight Center) as the standard star catalog. Some pre-process operations on the standard star catalog should be taken. Firstly, we should eliminate binary and variable stars from the SKYMAP catalog. Secondly, according to the sensitive ability of CCD or

APS sensor, we should set a magnitude limit to an appropriate value to ensure all selected guide stars can be imaged by the sensor and also can reduce the number of guide stars in the subset catalog [9].

In order to enhance the speed of the accessing star catalog, we divided the celestial sphere into several blocks in declination direction. In this paper, the size of FOV is $12^\circ \times 12^\circ$. So we selected the interval of block size is 3° and the whole celestial sphere is divided into $(90 - (-90)) / 3 = 60$ blocks. If we give a random attitude pointing, the searching range of declination just occupies 5 blocks. So the speed of searching the star catalog is 1/12 of traditional searching range. Because the circle of right ascension is not evenly, we propose a method to calculate the range of right ascension when we know the declination and the size of FOV.

Suppose the random attitude pointing is (C_{J_0}, C_{W_0}) at right ascension and declination respectively. The half size of FOV is R degree. Then the range of declination is C_W ($C_{W_0} - R, C_{W_0} + R$). The right ascension calculation is not simple like that. The range of right ascension increases along with the declination grows. So we use the upper limit of the declination $C_{W_0} + R$ to calculate the upper limit of right ascension. The calculation range of right ascension is described in Figure 4.

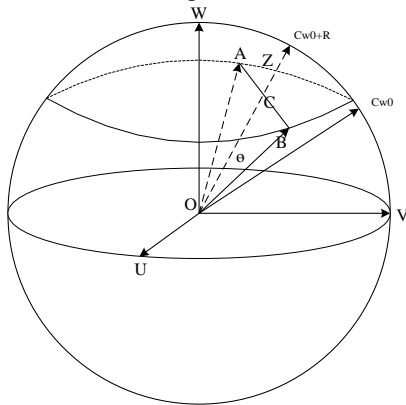


Figure 4 The calculation range of right ascension
The range of right ascension can be calculated as follows:

$$C_J \in (C_{J_0} - \arctan(\tan \theta / \cos(C_{W_0} + R)), C_{J_0} + \arctan(\tan \theta / \cos(C_{W_0} + R))) \quad (1)$$

The criterion of stars in the FOV is given as follows:

$$\begin{aligned} \alpha_i &\in C_J \quad (i = 1, 2 \dots n) \\ \delta_i &\in C_W \quad (i = 1, 2 \dots n) \end{aligned} \quad (2)$$

$$R > \phi = \arccos\left(\frac{\vec{i} \cdot \vec{p}}{|\vec{i}| |\vec{p}|}\right) \quad (i = 1, 2 \dots n)$$

where (α_i, δ_i) is guide star's right ascension and declination. n is the number of guide stars in the 5 blocks. \vec{p} is the boresight reference vector in celestial coordinate. \vec{i} is the guide stars reference vectors in celestial coordinate. R is the half size of FOV. (\bullet) is the

dot product operation. ϕ is the separation angular distance between boresight vector and guide star vector.

Firstly, we use the range of declination to determine which 5 blocks (sub catalog) should be searched, suppose n stars in these 5 blocks. Secondly, using the dot product in equation (2) between boresight reference vector \vec{p} and n stars' vector to determine which star is in FOV. If n stars are all operated in dot product, it is time-consuming. We use the range of right ascension given by equation (1) to further reduce the number of stars searched in star catalog. The method can accelerate the speed of the accessing star catalog.

B. Coordinate transformation

The simulated star image needs to calculate the guide star positions on the 2-D CCD plane. So the coordinate transformation is the first task of star image simulation. The guide star position in the celestial sphere is given by α_i (right ascension) and δ_i (declination) (from the SKYMAP catalog). This position is in the celestial coordinate system (CCS), which is centered of the earth. The X-axis points at the mean equinox. The Z-axis points at the celestial pole. The Y-axis is constructed the right-hand system with the X and Z-axis. The guide star vector given by α_i and δ_i can be transformed into the 3D coordinate in CCS and can be shown as [10]:

$$[U, V, W]^T = [\cos \alpha_i \cos \delta_i, \sin \alpha_i \sin \delta_i, \sin \delta_i]^T \quad (3)$$

Guide star positions on the CCD coordinate system are needed. The center of the CCD coordinate system is the lens focus. The Z-axis points at the boresight direction of the star sensor. The X-axis is parallel to the rows direction of pixels of the CCD plane. The Y-axis is also constructed the right-hand system with the X and Z-axis. The guide star positions $[X, Y, Z]$ in CCD coordinate system is given by [11]:

$$[X, Y, Z]^T = M[U, V, W]^T \quad (4)$$

The matrix M is the rotation matrix from CCS to the CCD coordinate. A 3-2-1 Euler angle rotation is adopted. It rotates an angle ϕ round the Z-axis first. Then rotating an angle θ round the Y-axis and finally rotating an angle φ round the X-axis. The frame of coordinate transformation is shown in Figure 5.

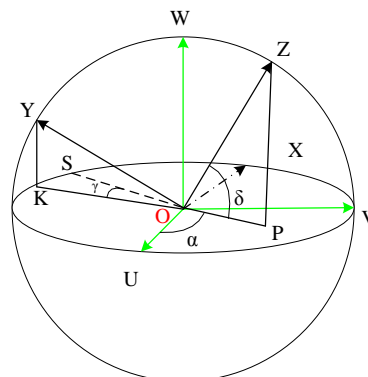


Figure 5 The frame of coordinate transformation

After the 3-2-1 rotating, we can get the rotation matrix M as follows [11]:

$$M = \begin{bmatrix} 1 & 0 & 0 \\ 0 & \cos\varphi & \sin\varphi \\ 0 & -\sin\varphi & \cos\varphi \end{bmatrix} \begin{bmatrix} \cos\theta & 0 & -\sin\theta \\ 0 & 1 & 0 \\ \sin\theta & 0 & \cos\theta \end{bmatrix} \begin{bmatrix} \cos\phi & \sin\phi & 0 \\ -\sin\phi & \cos\phi & 0 \\ 0 & 0 & 1 \end{bmatrix} \quad (5)$$

$$= \begin{bmatrix} \cos\theta\cos\phi & \cos\theta\sin\phi & -\sin\theta \\ \sin\varphi\sin\theta\cos\phi - \cos\varphi\sin\phi & \sin\varphi\sin\theta\sin\phi + \cos\varphi\cos\phi & \sin\varphi\cos\theta \\ \cos\varphi\sin\theta\cos\phi + \sin\varphi\sin\phi & \cos\varphi\sin\theta\sin\phi - \sin\varphi\cos\phi & \cos\varphi\cos\theta \end{bmatrix}$$

where $\varphi = \delta$, $\theta = -\delta$, $\phi = \gamma$

substituting equation (3) and (5) into (4), yields

$$\begin{aligned} X &= \sin\delta\sin\delta_i + \cos\delta\cos\delta_i\cos(\alpha - \alpha_i) \\ Y &= -\sin\gamma\sin\delta\cos(\alpha - \alpha_i) + \cos\gamma\cos\delta_i\sin(\alpha_i - \alpha) \\ &\quad + \sin\gamma\cos\delta\sin\alpha_i\cos\delta_i \\ Z &= -\cos\gamma\sin\delta\cos(\alpha - \alpha_i) + \sin\gamma\cos\delta_i\sin(\alpha - \alpha_i) \\ &\quad + \cos\gamma\cos\delta\sin\delta_i \end{aligned} \quad (6)$$

Normalizing the equation (6), we can get the guide star position [x,y] on the 2-D CCD plane.

$$\begin{aligned} x &= f \times \frac{Y}{X} \\ y &= f \times \frac{Z}{X} \\ f &= \frac{n}{2} \times \frac{1}{\tan(FOV / 2)} \end{aligned} \quad (7)$$

where the f is the lens focus, FOV is the size of field of view (in this paper is $12^\circ \times 12^\circ$). n is the row or column number of pixels of CCD. Through the equation (7), we can get the star position on the 2D CCD plane to generate the simulated star image.

C. Star magnitude simulation

Star magnitude is important information on simulated star image. The visible magnitude of the stars is given by the SKYMAP catalog. The magnitude of stars is close related with the irradiance of stars and can be calculated as follows [12]:

$$m_i = -2.51 \lg \frac{E_i}{E_0} \quad (8)$$

where E_0 is the irradiance energy of star with magnitude 0, E_i is the irradiance energy of star i, m_i is the magnitude of star i.

If we want simulate magnitude 0~6.5, the irradiance difference ratio between magnitude 0 and 6.5 should larger than 100. But the computer gray level is limited and can't reach the 100 ratio. We use the linear relationship between magnitude and gray level to simulate the magnitude of stars and are given as follows:

$$G_i = 10 \times (m_{\max} - m_i) + G_{\min} \quad (9)$$

where m_{\max} is the maximum magnitude can be simulated (in this paper $m_{\max} = 6.5$), G_{\min} is the gray value according to the m_{\max} ($G_{\min} \in (120 \sim 160)$), m_i is the magnitude of star i, G_i is the gray value of star i.

After getting the simulated gray value of star, we should consider the distribution of star energy. If the star energy concentrate on one single pixel, then we can't use the centroid algorithm to calculate subpixel accuracy star position. So the star sensor camera should be defocused slightly in order to spread the starlight energy over several neighbor pixels. If a small displacement δ_z from the image plane, the star energy distribution area will increase and its diameter is [13]:

$$D = \frac{\delta_z}{F\#} \quad (10)$$

where the F# is the optics number of the image sensor. The unit of the D is μm .

After defocusing, the starlight signal intensity distribution spread point function is reasonable approximated by the Gaussian function and the 2-D situation function can be written as [14]:

$$f(x, y) = \frac{k}{2\pi\sigma^2} \exp\left[-\frac{(x-x_c)^2 + (y-y_c)^2}{2\sigma^2}\right] \quad (11)$$

where (x, y) is the valid neighbor pixels positions, (x_c, y_c) is the accuracy star position on the CCD plane, σ is the dispersion radius of the star intensity. Figure 6 is the simulation of single star point under consideration of defocus and Gaussian energy distribution.

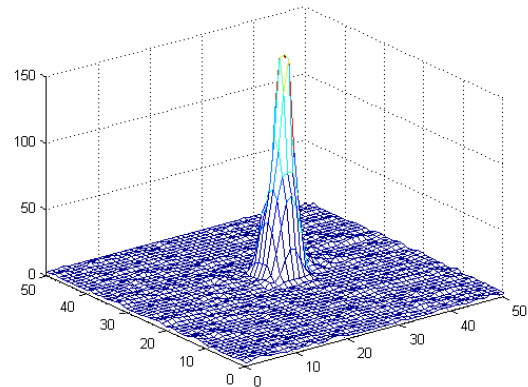


Figure 6 Star point simulation under 7×7 diameter

D. Noise and Sky environment simulation

Actually, the star image can be completed by the former three parts. In order to provide the noisy star image to test the stability of star sensor, we take full consideration of noise and sky environment effects in the star image simulation.

Typically in simulation, the noise is used the white Gaussian noise with zero mean and some value in standard deviation. In the star image simulation, we can add the white Gaussian noise on the positions of stars and the magnitude of stars.

Nebula and Cluster is also a disturbance factor which can influence the operation of star sensor. Once the nebula or the cluster enters into the FOV, it will cover some useful stars because of its diameter is much bigger than single star. The Messier catalog [15] provides the information about the nebula and the cluster in the sky. There are about 110 nebulas in the sky, but only 35 nebulas can be detected by the CCD detector. The Messier catalog gives out the position and diameter of the nebulas.

First, we can calculate the number of occupied pixels per degree. The CCD size is 512×512 pixels, the FOV is $12^\circ \times 12^\circ$, then the occupied pixels per degree is calculated as follows:

$$\frac{512 \times 25}{(12^\circ / 2)} = \frac{P \times 25}{(1^\circ / 2)} \quad (12)$$

$P=64$ pixels/degree

The Messier catalog give out the diameter of the nebula, suppose one nebula width is W and Height is H , then the apparent diameter of the nebula in image is:

$$\begin{aligned} Row_size &= (W / 60) \times 64 \\ Column_size &= (H / 60) \times 64 \end{aligned} \quad (13)$$

where the Row_size and $Column_size$ are the number of pixels occupied by the nebula on CCD plane.

The moon lights entering the FOV is also taken into account, it can be simulated by circle or ellipse shape.

IV. ZENITH OBSERVATION ALGORITHM

The star image simulation test system is described above. It just can test the star recognition rates and the software stability of the star sensor. It is necessary to design the semi-physical test system to test the accuracy of the star sensor. The semi-physical test system captured the stars from the real night sky. Night sky experiments usually use the high accuracy telescope to point one direction and fixed the star sensor on it to calculate the attitude of the direction pointed by the telescope. Under the condition of without telescope, we proposed a new zenith observation method to test the accuracy of star sensor.

The zenith method takes the earth as an evenly rotational turntable. It needs high accuracy spirit level to make sure the star sensor points at the zenith direction. The star sensor captured the stars from the zenith direction and calculated the attitude. Then, we use the astronomy knowledge to figure out the zenith position at the shooting time. Compared the star sensor's attitude with the zenith ideal attitude, we can test the accuracy of the star sensor without telescope.

Before using the zenith method, we should know two input parameters, the shooting time (UTC) and the location of star sensor (geographical latitude, geographical longitude and geographical Height in geocentric coordinate system). The output is the zenith position in the conventional inertial system. The flow of the coordinate transformation is described in Figure 7.

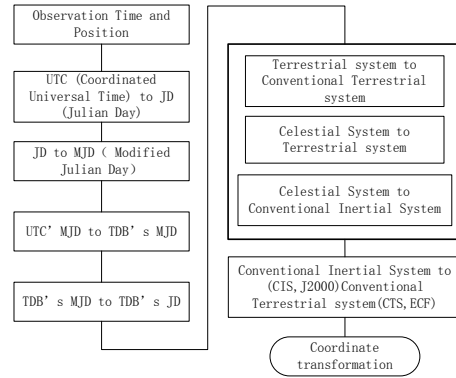


Figure 7 The flow of Zenith observation algorithm

The zenith observation algorithm also can be written by [16]:

$$[CIS] = Q(t)R(t)W(t)[CTS]S(t) \quad (14)$$

CIS: Conventional Inertial System

CTS: Conventional Terrestrial System

$S(t)$: the transformation matrix from the geocentric coordinate system to CTS.

$W(t)$: the transformation matrix from CTS to Terrestrial System (TS) consideration of the polar motion effects

$R(t)$: the transformation matrix from TS to Celestial System (CS), from the rotation of the Earth around the axis of the pole.

$Q(t)$: the transformation matrix from CS to CIS under consideration of the precession and nutation.

The matrix described above needs a lot of observation information released by International Astronomical Union (IAU) every year, and the calculating doesn't mention in detail in this paper.

V. EXPERIMENTS AND RESULTS

In this section, we design a number of experiments to verify the laboratory test system designed in this paper. The experiments are divided into two parts, the simulated star image test and the semi-physical test.

A. Simulated star image test

Star image simulation uses the software to simulate the star image captured by the CCD sensor. The theory of the star image simulation is described in the section III. With the parameters of FOV is $12^\circ \times 12^\circ$, focal length f is 60.89 mm, pixel size is 25um, image plane size is 512×512 . We give out 4 types of simulations: original star image simulation without noise, noisy star image simulation, nebula simulation, moon lights entering the FOV simulation. Those simulation results are shown in the Figure 8 to Figure 11.

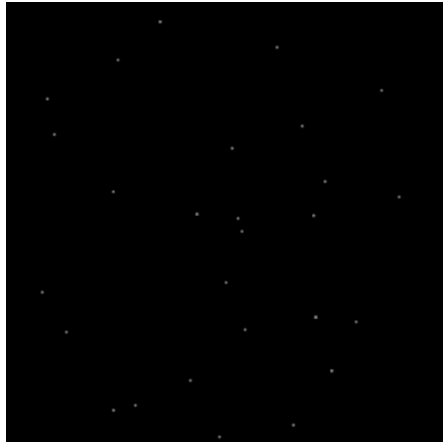


Figure 8 Original star image simulation without noise pointing at (-130,-60,90)

In Fig. 8, the star image pointing at the (-130,-60,90) is simulated. It is shown that the simulated star image method is validated and can be used to test the star sensor.

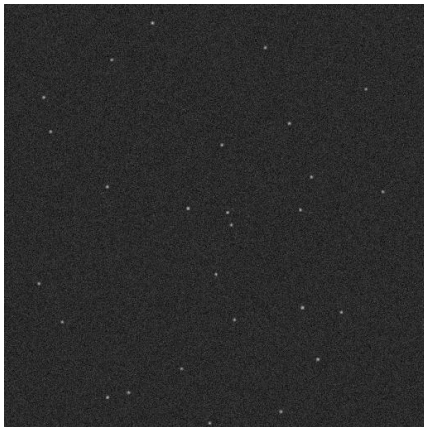


Figure 9 Noisy star image simulation with adding white Gaussian noise

In Fig. 9, the white Gaussian noise is added into the simulated star image. It can be used to test the stability of star sensor software.



Figure 10 The nebula simulation in the simulated star image

In Fig. 10, the nebula is simulated in the star image. The nebula is M33 (in the Messier catalog) with position at (23.475, 30.65), so the boresight of the star sensor is selected at (26,33,90). This simulation is considered the sky environment effects on star sensor operation.



Figure 11 The moon lights entering FOV simulation

In Fig. 11, we simulated the moon lights entering into the star sensor FOV. The moon can affect the operation of the star sensor. The simulation can test the star recognition rate, when the star sensor under the stray light entering into the FOV.

We also selected 1000 random attitudes adding white Gaussian noise on star magnitude from 0.1 to 0.6 to test the performance of star sensor. It took 0.4 second to complete one image processing and the star identification success rate under the noise lower than 0.3 magnitude was 98.6%. Once the LISA is success, the star sensor can enter the tracking mode quickly. When the magnitude higher than 0.4, the success rate of star recognition has a little decrease. The experiments results showed that the star sensor software was stable and insensitive to the magnitude noise. It also demonstrated that the star image simulation test system is feasible.

B. Semi-physical experiments

Except the simulated star image test, we also take experiments in real night sky. The night sky experiments were carried out on NAOC's observation station in XingLong, Hebei Province, in December 2009. We took about 900 images under different orientations and different noises. A real sky image captured by the star sensor and its 3D processing is given in Figure 12 and 13.



Figure 12 A real sky image captured by star sensor

Table 1 The data using zenith method to test the accuracy of star sensor

Index	Photo time						Ideal RA	Ideal Declination	Calculated RA	Calculated Dec
IMG_599	2009	12	14	22	54	47	64.50938087	40.18066423	64.7728172	40.45749233
IMG_600	2009	12	14	22	54	51	64.52608685	40.18067916	64.7909947	40.45777087
IMG_601	2009	12	14	22	54	55	64.542793	40.1806941	64.80881278	40.45855001
IMG_602	2009	12	14	22	55	0	64.56367565	40.18071278	64.82680278	40.45757764
IMG_603	2009	12	14	22	55	4	64.58038164	40.18072773	64.84569346	40.45808776
...
IMG_660	2009	12	14	22	59	43	65.74563994	40.1817753	66.014071	40.46061216
IMG_661	2009	12	14	22	59	48	65.76652276	40.18179417	66.03273553	40.46010127
IMG_662	2009	12	14	22	59	53	65.78740575	40.18181304	66.0537399	40.4601582
IMG_663	2009	12	14	22	59	58	65.80828874	40.18183191	66.07607295	40.46018708
IMG_664	2009	12	14	23	0	3	65.82917174	40.18185079	66.09627866	40.45950718

Figure 14 The relative attitude Error in Right Ascension

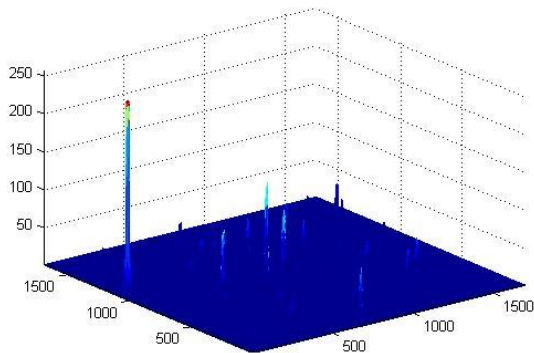
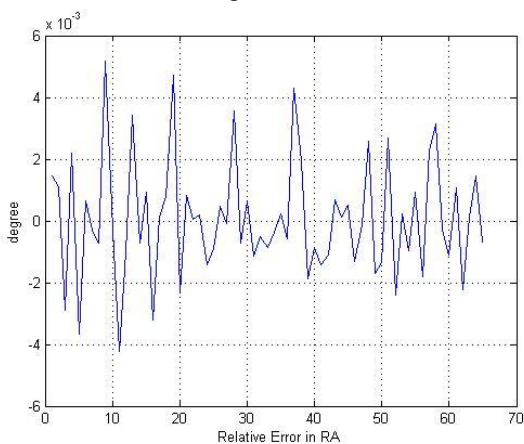


Figure 13 The 3D process of the real sky image

There are about 100 images pointing at the zenith in all real sky images. We selected 66 images to validate the zenith observation method and to test the relative accuracy of the star sensor. The ideal attitude figured out by the zenith method and the calculated attitudes provided by the star sensor about the 66 images are shown in table 1.

We can calculate the relative accuracy of the star sensor. The relative error in right ascension and declination are shown in Figure 14 and 15.



In Fig. 14, we can calculate the relative attitude error in right ascension using the data in table 1. The star sensor accuracy in right ascension is about $5 \times 10^{-3} \times 3600 = 18''$.

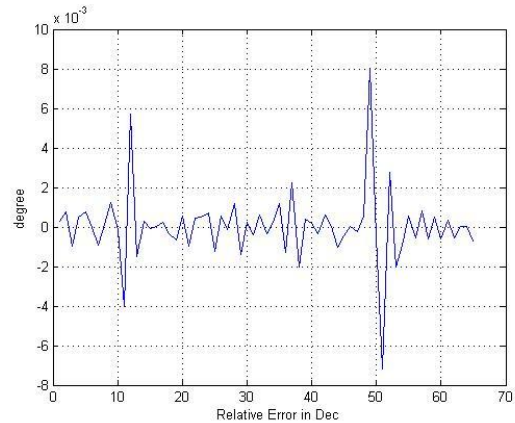


Figure 15 The relative attitude Error in Declination

In Fig. 15, we also can calculate the relative attitude error in Declination through the data in table 1. The star sensor accuracy in declination direction is about $9 \times 10^{-3} \times 3600 = 32''$.

Through the experiments above, we can see that the zenith method can meet the accuracy testing requirements of the star sensor without telescope. The laboratory test system designed in this paper is proved to be feasible and can meet the requirements of performance evaluation of the star sensor.

VI. CONCLUSIONS

A novel laboratory test system is designed in this paper. We give out two methods to evaluate the performance of star sensor, the simulated star image method and the zenith observation method. The star image simulation is described in detail, and the nebula and moon lights entering into the CCD FOV are taken into account. A fast accessing star catalog method is proposed. In the semi-physical test system, we proposed a new zenith method to

test the relative accuracy of the star sensor without using telescope. Experiments results prove our Laboratory test system is feasible and can meet the requirements of performance evaluation of the star sensor.

REFERENCES

- [1] C.C. Liebe. "Star trackers for attitude determination," IEEE Aerospace and Electronic Systems Magazine, 10 1995, pp. 10-16.
- [2] W. James Alexander, H. Daniel Chang, "Cassini Star Tracking and Identification Algorithms, Scene Simulation, and Testing," SPIE, vol. 2803, pp. 331-336, 1996.
- [3] J. Leif Jorgensen, A. Pickles. "Fast and robust pointing and tracking using a second generation star tracker," SPIE, vol. 3351, pp. 51-61, 1998.
- [4] J. Gwanghyeok. "Autonomous star sensing, pattern identification, and attitude determination for spacecraft: an analytical and experimental study," Doctor thesis, Texas A&M university, 2001.
- [5] P. oosthuizen, C. Collingwood, L. Saleem, C. Alexander and G. Scott. "Development and on-orbit results of the SSTL low cost commercial star tracker," AIAA Guidance, Navigation and Control conference and exhibit, 2006, pp. 1-11.
- [6] W. zhao-kui, Z. yun-lin. "Design and implementation of star pattern simulator for use of space surveillance," Journal of System Simulation. Vol.18 (5), pp. 1195-1211, 2006.
- [7] H. yi-ning, G. Yan. "Design and realization of a dynamic display algorithm for star map," Journal of Astronautics, Vol.29(3), pp. 849-853, 2008.
- [8] R. Giancarlo. M. Antonio. "Laboratory test system for performance evaluation of advanced star trackers," J Guid Control DYN 25(2), pp. 200-208, 2002.
- [9] J. Jiang, G. J. Zhang, X. G. Wei, X. Li, "Rapid star tracking algorithm for star tracker," IEEE Aerospace and Electronic Systems Magazine, vol. 24, pp.23-33, 2009.
- [10] J. Yang, T. Zhang, J.Y. Song, B. Liang, Q.Q. Ding. "The Algorithm Research of Ground Celestial Sphere and Dynamic Star Simulator", Journal of system simulation, Vol.22, pp. 202-206, 2010.
- [11] Z. jun-ping, L. Tao, Z. jian-lin and Q. guo-hui. "A method of CCD star image simulation," Chinese space science and technology, Vol.3, pp. 46-50, 1999.
- [12] C. Harry strunz, B. Troy and D. ethridge. "Estimation of stellar instrument magnitudes," SPIE, vol.1949, pp. 228-235, 1993.
- [13] G. Rufino, D. Accardo. "Enhancement of the centroiding algorithm for star tracker measure refinement," Acta Astronaut, vol.53, pp.135-147., 2003.
- [14] Katake, A.B. "Modeling, image processing and attitude estimation of high speed star sensors," Doctor thesis, Texas A&M university, pp.33-37, 2006.
- [15] <http://202.112.85.100/aobn/resource.htm> (accessed on 9 October 2010).
- [16] http://www.iers.org/nn_11216/SharedDocs/Publikationen/EN/IERS/Publications/tm/TechnNote32/tm32,templateId=raw,property=publicationFile.pdf/tm32.pdf (accessed on 30 June 2010).

Jun yang and is currently a Ph.D. candidate in the Department of Automation at Tsinghua University. He has received his B.S. degree in automation from

Northwestern Polytechnical University, China, in 2004, received Master from Beijign University of Posts and Telecommunications in 2007. His research interests include star sensor technology, Micro-Satellite technology and artificial intelligence.

Bin Liang is a Professor in the Department of Automation at Tsinghua University. He received his Ph.D. degree in Precision Instrumentation and Machinery from Tsinghua University, China, in 1994. His research interests include Micro-Satellite technology and space robotics.

Tao Zhang is an Associate Professor in the Department of Automation at Tsinghua University. He received his B.S., M.S. and Ph.D. degrees in Electrical Engineering from Tsinghua University, China, in 1993, 1995 and 1999, respectively. He received his second Ph.D. degree in Electrical Engineering from Saga University, Japan in 2002. His research interests include robotics and system control engineering.

Jing-yan Song is a Professor in the Department of Automation at Tsinghua University. He received his Ph.D. degree in Systems Engineering and Engineering Management from The Chinese University of Hong Kong, China, in 1998. His research interests include Micro-Satellite technology, intelligent transportation system and space robotics.

Liang-liang Song is currently a Master in the Department of Automation at Tsinghua University. He has received his B.S. degree in automation from Shan Dong University, China, in 2008. His research interests include star sensor technology, Micro-Satellite technology.